Construction of g-C_3N_4/Ag/TiO_2 composite microspheres with enhanced photoelectric performance in dye-sensitized solar cells

Haoran Yan[1,a], Guoqiang Yang[1,b], Jianxin Wang[1,c], Bo Feng[1,d], Ke Duan[1,e], Jie Weng[1,f]

1. School of Materials Science and Engineering, Southwest Jiaotong University, Chengdu 610031, Sichuan, PR China.
[a]h.r.yan@my.swjtu.edu.cn, [b]984184669@qq.com, [c]jwang@swjtu.edu.cn, [d]fengbo@home.swjtu.edu.cn, [e]keduan2@gmail.com, [f]jweng@swjtu.edu.cn

Keywords: DSSCs, g-C_3N_4, TiO_2 microspheres, Ag, photoelectric conversion efficiency

Abstract. In the present work, a novel heterostructured dye-sensitized solar cell (DSSC) was fabricated by using simple spin-coating steps. g-C_3N_4 and Ag modified TiO_2 microspheres were used as the photoanode materials. The aim of this study was to modify TiO_2 microspheres by using g-C_3N_4 so as to retard the recombination of electron-holes and in turn to improve the photoelectric conversion efficiency (PCE) of DSSCs. Additionally, Ag nanoparticles were photodeposited as the interlayer between g-C_3N_4 and the surface of TiO_2 microspheres to increase visible-light absorption via the surface plasmon resonance, so as to further improve the PCE of DSSCs. The experimental results showed that the performance of DSSCs was obviously improved after modified by g-C_3N_4 and Ag.

1. Introduction

A The dye-sensitized solar cells (DSSCs) have been attracting considerable attention due to their high photoelectric conversion efficiency (PCE) and low cost, and the photoelectric conversion efficiency of DSSCs are also continuously being improved [1,2]. However, the recombination between electrons and electrolyte is becoming a big challenge to achieve a higher solar cell performance [3-5]. Hence, the approach by using suppressing electron recombination is becoming an effective way to enhance the performance of solar cells. Recently, much interest has been focused on graphene-doped TiO_2, which is used to extend light absorption to the visible-light region and meanwhile to effectively prevent the migration of electrons from TiO_2 to the electrolyte [6,7].

g-C_3N_4 has the special graphite-like electronic band structure and high thermal stability and chemical stability and compared with graphene, g-C_3N_4 can be more easily prepared by the thermal condensation by using low-cost precursors, thus, it might become a potential material to substitute for grapheme which is playing a role in the application of dye-sensitized solar cells [8].

In this work, a facile method was developed to fabricate a novel multistage structure DSSC, which consisted of Ag and TiO_2/g-C_3N_4 mesoporous microspheres. The resultant g-C_3N_4 thin layer on TiO_2 surface was used to promote the electron transport by retarding the backward recombination of electrons from TiO_2 and electrolyte, and to contribute additional electrons transferred from the CB of g-C_3N_4 to the CB of TiO_2. Additionally, Ag was used as the interlayer between g-C_3N_4 and the surface of TiO_2 to increase visible-light absorption via the surface plasmon resonance [9] and the transport of the separated electrons, so as to enhance the performance of DSSCs. This novel multistage structure would be expected to achieve a higher performance of solar cells.

2. Experimental

Preparation of protonation g-C_3N_4 sheets. g-C_3N_4 nanosheets were synthesized on the basis of a procedure reported previously [8,9]. Specifically, 15 g of urea was added into a crucible with a cover, and then the crucible was placed into a Muffle furnace and heated at 520 ^oC for 4 h with a temperature ramping rate of 25 ^oC/min. The obtained light yellow agglomerate was ground into powder. 1.0 g of the g-C_3N_4 powder was treated with HCl (18.5 wt %, 50 mL) for 5 h at room temperature for protonation. Before being filtered, the suspension was diluted, and then the protonated g-C_3N_4 was

washed with deionized water and dried. A well-dispersed aqueous solution of 1 mg/mL was obtained by ultrasonic dispersion in deionized water for 30 min.

Preparation of g-C_3N_4/Ag/TiO_2 composite microspheres. Pure TiO_2 microspheres (denoted as CAT-0) were prepared by a sol-gel method using titanium isopropoxide as a precursor according to a previous report [10]. The as-prepared TiO_2 microspheres (300 mg) were mixed with 200 mL of deionized water under ultrasonication for 30 min. Then, 1.0 mL of 5% polyethylene glycol (PEG) 2000 solution was added and the dispersion was stirred for 10 min. For deposition of silver on the surface of TiO_2 microspheres, a photodeposition method was applied as follows: 3.5 mL of $AgNO_3$ solution (2.754 mg/mL) was added to the dispersion. Then the suspension was transferred to a water-cooled reactor (250 mL) and irradiated under a PLS-SXE300 Xe lamp with 100 mW/cm^2 illumination intensity for 60 min. The theoretical value of the amount of loaded Ag was 2 wt%. To wrap g-C_3N_4 on Ag/TiO_2 microspheres, a certain amount (9, 15 and 24 mL) of the protonated g-C_3N_4 sheet solution (1 mg/mL) was added and the temperature was kept at 70 ^oC for 60 min. The resulting suspension was filtered, washed with deionized water three times and dried at 60 ^oC for 24 h in a vacuum oven. The theoretical wrapping amount of g-C_3N_4 was 3, 5 and 8 wt % (denoted as CAT-3, CAT-5, CAT-8), repectively.

Fabrication of devices. The photoanodes were prepared as follows. TiO_2 and CAT pastes were prepared according to a common method [11]. The films were prepared by the spin-coating method. FTO glass (NSG, 7 Ω/sq) was cut into the desired dimensions (1.2 cm × 1.8 cm) and cleaned with mild detergent, distilled water and subsequently with ethanol and acetone in an ultrasonic bath for 15 min, respectively, and then dried for use as the substrate. Firstly, the TiO_2 blocking layer was deposited on the clean substrates by spin-casting at 2500 rpm using 200 mM titanium diisopropoxidebis (acetylacetonate) solution in ethanol for 30 s and then sintered at 450 °C for 30 min in air. Subsequently, the TiO_2 layer with a thickness of about 6~8 μm was prepared by coating the TiO_2 paste containing P25 nanoparticles on the blocking layer also by using a spin-coating technique at 3000 rpm for 30 s, and then sintered at 450 ℃ for 30 min in air. The last step was repeated using the previous method to obtain alight scattering layer composed of the as-prepared CAT paste, and then calcined at 500 °C in Ar atmosphere for 30 min. The film thickness was ~15 μm. For comparison, an electrode was also prepared by using pure TiO_2 and microspheres without g-C_3N_4. Finally, after natural cooling to room temperature, the TiO_2 films were soaked in the 40 mM $TiCl_4$ aqueous solution at 70 °C for 30 min and then were annealed at 450 °C for 15 min. Dye loading was performed by immersing the TiO_2 anode in a 0.3 mM dye N719 ethanol solution for 12 h. After the dye absorption, the samples were rinsed with ethanol, dried in N_2 atmosphere and then used as photoanodes for DSSCs. DSSCs were assembled in a typical sandwich-type cell by placing a platinum counter electrode on the electrode and the electrolyte was injected. The active area of the cells was 5×5 mm^2.

Characterization. X-ray diffraction (XRD) analysis of TiO_2 microspheres and composites was performed using a Philips X'Pert PRO X-ray diffractometer with a Cu Kα radiation (λ=1.5418 Å). The Fourier transform infrared spectra (FT-IR) of the samples were recorded using a FT-IR spectrometer (Shimadzu Corp., Tokyo, Japan). Surface morphologies of CATs were conducted using a field emission scanning electron microscopy (FESEM, JSM-7500F, Japan, JEOL). Diffuse reflectance spectrum of the samples were recorded with a UV–vis spectrophotometer (UV-2550, Shimadzu, Japan). Photovoltaic parameters of the DSSCs under a simulated AM 1.5G illumination with a light intensity of 100 mW/cm^2 provided by 150 W Xenon Arc Lamp (XBO 150 W/CROFR,OSRAM, USA) were measured with the aid of a potentiostat (CIMPS-2, Zahner, Germany).

3. Results and discussion

Phase structures. XRD patterns of g-C_3N_4 powders, TiO_2 microspheres after hydrothermal treatment, g-C_3N_4 modified TiO_2 microspheres and CAT-5 are shown in Fig.1A. After hydrothermal

treatment the crystallization of TiO_2 microspheres could be detected and all the diffraction peaks for TiO_2 and CNTs were assigned to the anatase phase of TiO_2 (JCPDS, no. 21-1272). It can be noted that no typical diffraction peaks corresponding to g-C_3N_4 or Ag could be observed in the XRD pattern of g-C_3N_4/TiO_2, Ag/TiO_2 and CAT-5 composite microspheres, probably due to very low weight amount of g-C_3N_4 or Ag compared with that of crystalline TiO_2 microspheres.

FT-IR spectra. The FT-IR spectra of the pure TiO_2 microspheres, g-C_3N_4, CAT-5 is shown in Fig.1B. For pure TiO_2 nanoparticles, a wide absorption band appearing at 500−700 cm^{-1} is attributed to Ti−O stretching. The peak appearing at 1624 cm^{-1} is attributed to the bending vibration of O−H [9]. The pure g-C_3N_4 shows the similar results to that described in previous report. As shown in Fig.1B, the absorption band at 1641 cm^{-1} can be ascribed to the C−N heterocyclic stretching vibration modes, whereas the four strong peaks at 1254, 1329, 1416 and 1572 cm^{-1} can be assigned to aromatic C−N stretching vibration modes [8]. Furthermore, it can be evidently shown that all of the main characteristic peaks of g-C_3N_4 and TiO_2 appeared in g-C_3N_4/TiO_2 composites. The results show that a condensation reaction between NH- groups on g-C_3N_4 and hydroxyl groups on TiO_2 nanoparticles was conducted.

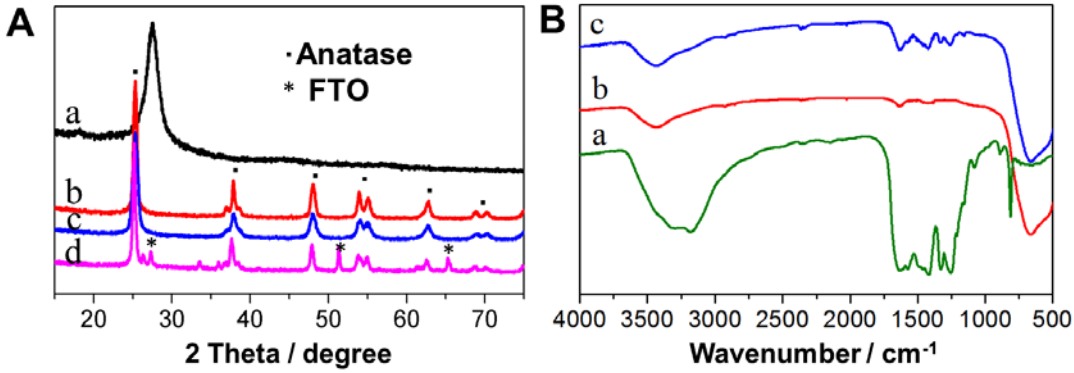

Fig. 1 (A) XRD patterns of (a) g-C_3N_4, (b) pure TiO_2 microspheres, (c) CAT-5 and (d) the anode film prepared by using CAT-5; (B) FTIR spectra of (a) g-C_3N_4, (b) TiO_2, (c) CAT-5.

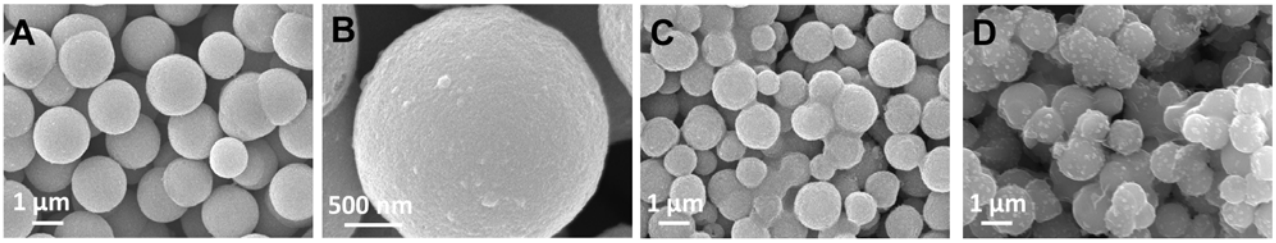

Fig. 2 (A, B) SEM images of TiO_2 microspheres before hydrothermal processing; (C) TiO_2 microspheres after hydrothermal processing; (D) g-C_3N_4 modified TiO_2 microspheres after hydrothermal processing.

Morphology characterization. The FE-SEM images show that the as-synthesized TiO_2 microspheres before hydrothermal processing are regular and uniform with an average diameter of about 1.8 μm (Fig. 2A,B), which possess very smooth surfaces. After hydrothermal treatment, shrinkage and comparatively rough surfaces were produced (Fig. 2C). Fig. 2D indicates that TiO_2 microspheres have been wrapped by g-C_3N_4 nanosheets.

UV-vis spectra. Fig. 3 shows the UV-Vis diffuse reflectance spectra of the pure g-C_3N_4 and CAT composites microspheres. The absorption edge at 400~450 nm for pure g-C_3N_4 corresponds to the intrinsic band gap of g-C_3N_4 (~2.7 eV) [12]. For all the composites samples, the sharp absorption increase at wavelengths shorter than 380 nm is due to the intrinsic band gap absorption of anatase TiO_2. Particularly, compared to the pure TiO_2 microspheres sample, the composites (CAT-3, CAT-5, CAT-8) exhibit a obviously enhanced visible-light absorption in a wavelength range of 400-450 nm, owing to the lower band gap by loading g-C_3N_4, further confirming the successful loading of g-C_3N_4 on the TiO_2 microsphere surface.

Photoelectric performance characteristics. In order to get an optimal structure to achieve a good photoelectric performance for DSSCs, the investigation of the effect of CATs microspheres on the

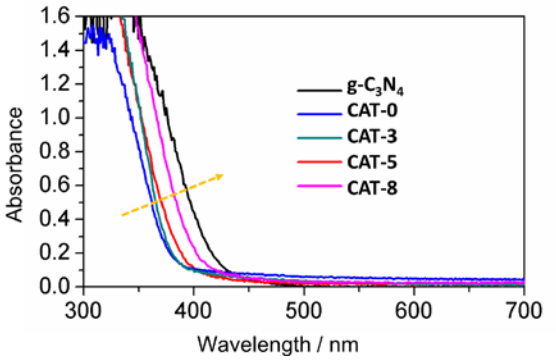

Fig.3 UV-vis diffuse reflectance spectra of g-C_3N_4 and the CAT-0, CAT-3, CAT-5, CAT-8 composites.

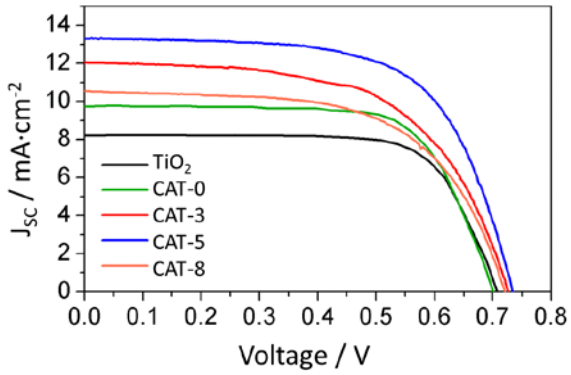

Fig.4 Comparison of the I-V characteristics of DSSCs made from pure TiO_2 nanoparticles, CAT-0, CAT-3, CAT-5 and CAT-8.

PCE of DSSC was conducted. It can be seen from Fig.4 that the DSSCs with g-C_3N_4 and Ag modified microspheres exhibited much better performance compared with the DSSC only with pure TiO_2 microsphere light scatting layer, and that the PCE of the DSSCs based on the g-C_3N_4 coated Ag-TiO_2 microspheres photoanodes are strongly dependent on the loaded amount of g-C_3N_4. The results showed that the PCE of the DSSCs with CAT-3, CAT-5, and CAT-8 was 5.45%, 6.43% and 4.85%, respectively. Among them, the DSSC with the CAT-5 light scatting layer exhibited the best performance, with J_{SC} =13.35 mA·cm^{-2}, V_{OC} =0.736 V, and FF = 0.654, which corresponded to a notably high PCE of 6.43 %, representing an improvement of about 41 % compared with the DSSC just using CAT-0 as the light scatting layer (PCE=4.57%). It is known well that in addition to the electron concentration, the electron diffusion is another important factor that can affect the performance of solar cell. It is possible that the overloading of g-C_3N_4 may partially cut off the effective connection among TiO_2, thus interrupting the fast transport of electrons from TiO_2 to FTO glass substrates and causing the decrease of J_{SC}. Due to co-effect of electron concentration and electron diffusion, the prepared DSSCs show first increase and then decrease performance tendency with increasing the loaded g-C_3N_4 amount. The best PCE of 6.43% was obtained for the DSSC based on CTS-5, which is about 1.6 times that for the DSSC based on pure TiO_2 nanoparticles (P25).

The mechanism of the performance improvement of DSSCs. Based on our results and the literatures, a possible charge transfer process for the g-C_3N_4/Ag/TiO_2 is proposed and schematically exhibited in Fig. 5. Here we assume that the thin layer of g-C_3N_4 formed on TiO_2 surface plays an important role in the improvement of the solar cell performance, which can act as the block layer to suppress the electron backward recombination with electrolyte [13,14]. The g-C_3N_4 has more negative CB position when compared with that of TiO_2, thus, the electrons in the CB of TiO_2 cannot transfer to g-C_3N_4. Contrarily, the photoinduced electrons from the CB of g-C_3N_4 will transfer to the CB of TiO_2. As a result, the g-C_3N_4 thin layer on TiO_2 surface can effectively promote the electron transport by retarding the backward recombination of electrons from TiO_2 and electrolyte, and also

contribute additional electrons to increase the electron concentration in the photoanodes. However, it is noted that a higher amount of g-C_3N_4 (CAT-8) obviously decreased the electron transport from the TiO_2 to FTO substrate. This is because the overloading of g-C_3N_4 should partially cut off the effective connection among TiO_2 [6], which interrupted the fast transport of electrons from TiO_2 to FTO glass substrates, resulting in the increase of electron transport resistance and the decrease of J_{SC}. Moreover, the nano-Ag depositing on the surface of TiO_2 microspheres played an important role as an electron-conduction bridge. The electrons transfer toward TiO_2 and electron-holes separation in g-C_3N_4 would be more efficient because of the formed Schottky barrier at the interface of Ag and TiO_2 nanoparticles [9,15]. On the other hand, the surface plasmon resonance of nano-Ag particles can enhance visible-light absorption, so as to further improve the performance of the DSSC.

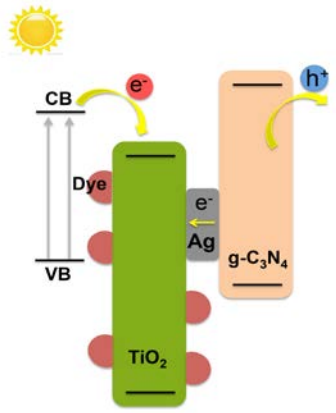

Fig. 5 Mechanism Scheme of g-C_3N_4 and Ag to increase the performance of DSSCs

4. Conclusion

In summary, g-C_3N_4 and Ag co-modified photoanodes were fabricated on FTO glass substrates by using spin-coating method. They were used as key materials in photoanodes of DSSCs and could significantly improve the performance of the DSSCs. g-C_3N_4 can retard the recombination of electron-holes and in turn to improve the photoelectric conversion efficiency (PCE) of DSSCs. Consequently, Ag nanoparticles were photodeposited as the interlayer between g-C_3N_4 and the surface of TiO_2 microspheres to increase visible-light absorption via the surface plasmon resonance, so as to further improve the PCE of DSSCs. A much higher PCE was found for the DSSC both with g-C_3N_4 and Ag modification (6.43%) compared to the DSSC based on pure TiO_2 nanoparticles (3.98%).

Acknowledgements

This work was supported by National Natural Science Foundation of China (No. 51072167 and No. 31370966) and the Fundamental Scientific Research Funds for Central Universities (SWJTU11CX058).

References

[1] B. O'Regan, M. Gratzel. A low-cost, high-efficiency solar cell based on dye sensitized colloidal TiO_2 films. Nature. Vol. 353 (1991) No.6346, p. 737-740.

[2] S. Mathew, A. Yella, P. Gao, et al. Dye-sensitized solar cells with 13% efficiency achieved through the molecular engineering of porphyrin sensitizers. Naut. Chem. Vol. 6 (2014) No.3, p. 242-247.

[3] J. Fan, S. Liu, J. Yu, et al. Enhanced photovoltaic performance of dye-sensitized solar cells based on TiO_2 nanosheets/graphene composite films. J. Mater. Chem. Vol. 22 (2012) No.33, p. 17027-17036.

[4] J.G. Yu, J.J. Fan, B. Cheng, Dye-sensitized solar cells based on anatase TiO 2 hollow spheres/carbon nanotube composite films. J. Power Sources. Vol. 196 (2011) No.18, p. 7891-7898.
[5] E. Palomares, J.N. Clifford, S.A. Haque, et al. Slow charge recombination in dye-sensitized solar cells (DSSC) using Al_2O_3 coated nanoporous TiO_2 films. Chem. Commun. Vol. 14 (2002) No.14, p. 1464-1465.
[6] H. Yan, J. Wang, B. Feng, et al. Graphene and Ag nanowires co-modified photoanodes for high-efficiency dye-sensitized solar cells. Solar Energy. Vol. 122 (2015), p. 966-975.
[7] J. S. Lee, K. H. You, C. B. Park. Highly photoactive, low bandgap TiO_2 nanoparticles wrapped by graphene. Adv. Mater. Vol. 24 (2012) No.24, p. 1084-1088.
[8] J. Xu, G. Wang, J. Fan, et al. g-C_3N_4 modified TiO_2 nanosheets with enhanced photoelectric conversion efficiency in dye-sensitized solar cells. J. Power Sources. Vol. 274 (2015), p. 77-84.
[9] Y Chen, W Huang, D He, et al. Construction of heterostructured g-C_3N_4/Ag/TiO_2 microspheres with enhanced photocatalysis performance under visible-light irradiation. ACS Appl. Mater. Inter. Vol. 6 (2014) No.16, p. 14405-14414.
[10] D. Chen, F. Huang, Y. B. Cheng, et al. Mesoporous anatase TiO_2 beads with high surface areas and controllable pore size: a superior candidate for high-performance dye-solar cells. Adv. Mater. Vol. 21 (2009) No. 21, p. 2206-2210.
[11] S. Ito, T. N. Murakami, P. Comte, et al. Fabrication of thin film dye-sensitized solar cells with solar to electric power conversion efficiency over 10%. Thin Solid Films. Vol. 516 (2008) No.14, p. 4613-4619.
[12] J. Low, S. Cao, J. Yu, et al. Two-dimensional layered composite photocatalysts. Chem. Commun. Vol. 50 (2014) No.74, p. 10768-10777.
[13] J. Liu, Y. Zhang, L. Lu, et al. Self-regenerated solar-driven photocatalytic water-splitting by urea derived graphitic carbon nitride with platinum nanoparticles. Chem. Commun. Vol. 48 (2012) No.70, p. 8826-8828.
[14] S. Cao, J. Yu. g-C_3N_4-based photocatalysts for hydrogen generation. J. Phys. Chem. Lett. Vol. 5 (2014) No.12, p. 2101-2107.
[15] B. Chai, T. Y. Peng, J. Mao, et al. Graphitic carbon nitride (g-C_3N_4)-Pt-TiO_2 nanocomposite as an efficient photocatalyst for hydrogen Production under visible light irradiation. Phys. Chem. Chem. Phys. Vol. 14 (2012) No.48, p. 16745 − 16752.